

# Novelty Detection Meets Collider Physics

Jan Hajer,<sup>1,2</sup> Ying-Ying Li,<sup>3,4</sup> Tao Liu,<sup>3</sup> and He Wang<sup>3</sup>

<sup>1</sup>*Institute for Advanced Studies, The Hong Kong University of Science and Technology,  
Clear Water Bay, Kowloon, Hong Kong S.A.R., P.R.China*

<sup>2</sup>*Centre for Cosmology, Particle Physics and Phenomenology,  
Université catholique de Louvain, Louvain-la-Neuve B-1348, Belgium*

<sup>3</sup>*Department of Physics, The Hong Kong University of Science and Technology,  
Clear Water Bay, Kowloon, Hong Kong S.A.R., P.R.China*

<sup>4</sup>*Kavli Institute for Theoretical Physics, University of California Santa Barbara, CA 93106-4030, USA*

Novelty detection is the machine learning task to recognize data, which belongs to a previously unknown pattern. Complementary to supervised learning, it allows the data to be analyzed in a model-independent way. We demonstrate the potential role of novelty detection in collider analyses using an artificial neural network. Particularly, we introduce a set of density-based novelty evaluators, which can measure the clustering effect of new physics events in the feature space, and hence separate themselves from the traditional density-based ones, which measure isolation. This design enables recognizing new physics events, if any, at a reasonably efficient level. For illustrating its sensitivity performance, we apply novelty detection to the searches for fermionic di-top partner and resonant di-top productions at LHC and for exotic Higgs decays of two specific modes at future  $e^+e^-$  collider.

## INTRODUCTION

Since its birth in 1950's [1], machine learning (ML) has evolved into a science addressing various *big data* problems. The techniques developed for ML, such as *decision tree learning* (DTL) [2] and *artificial neural networks* (ANN) [3], allow training computers to perform specific tasks usually deemed to be complex for simple handwoven algorithms. For *supervised learning*, the algorithm is first trained on distinct samples. Then the algorithm is able to classify the testing data into the classes defined at the training phase. In contrast, in *semi-supervised* and *un-supervised learning*, where partially labeled or unlabeled data is provided, the algorithm is expected to find the relevant patterns unassisted.

The last decade has seen a rapid progress in ML techniques, specifically the development of deep ANN. A deep ANN is a multi-layer network of threshold units [4]. Each unit computes only a simple nonlinear function of its inputs, which allows each layer to represent a certain level of relevant features. Unlike traditional ML techniques (e.g., Boosted Decision Trees) which rely heavily on expert-designed features in order to reduce the dimensionality of the problem, deep ANN automatically extract pertinent features from data, enabling data-mining without human knowledge. Fueled by vast amounts of big data, the fast development in training techniques and parallel computing architectures, modern deep learning systems have achieved major successes in computer vision [5], speech recognition [6], natural language processing [7], and recently emerge as a promising tool in scientific research [8–11], where the plethora of experimental data presents a challenge for insightful analysis.

High Energy Physics (HEP) is big data science and has a long history of using supervised ML for data analysis. Motivated by recent development in ML, pioneering

works have demonstrated the capability of deep ANN in understanding jet substructure [12–15], identification of particles [16], or even whole signal signatures (see, e.g. [17], where weakened supervised learning is applied). But, the primary goal of HEP experiments is to detect physics beyond the Standard Model (BSM), known or unknown, to establish the underlying fundamental laws of the nature. Despite of its significant role in current data analysis, supervised ML techniques suffer from the model dependence introduced during training. This problem potentially can be addressed by the techniques developed for *novelty detection* (for a review, see, e.g., [18]). Novelty detection is the task to recognize data, which belongs to an unknown pattern. If being interpreted as novel signal, BSM physics could be detected without specifying an underlying theory or utilizing model-dependent information during data analysis (except the sensitivity interpretation), using the relevant techniques. A combination of novelty detection and supervised ML thus may lay out a framework for the future HEP data analysis.

Some efforts related or partially related to this, though few and preliminary, have been made either at jet level [19, 20], or at event level [21–26]. To efficiently fulfill this task, a crucial step is to properly design the novelty evaluators, which enable evaluating the novelty of the data collected in experiments. Generally speaking, the design of the novelty evaluators defines the frontier of novelty detection [18]. In this letter, we propose a new set of density-based novelty evaluators. Different from traditional density-based ones which quantify isolation of the testing data from the known pattern, the new novelty evaluators measure the clustering effect of the testing data. Based on this, we design algorithms for novelty detection using an autoencoder, and then apply them to the sensitivity analysis of benchmarks at LHC and future  $e^+e^-$  colliders.

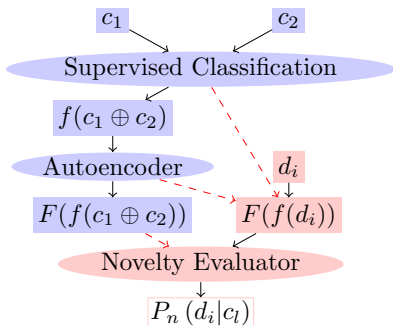


FIG. 1: The algorithm designed for novelty detection. The training and testing phases are marked in blue and red, respectively. Datasets, algorithm and probabilities are indicated by rectangular, elliptic and plain nodes, respectively. The information gathered during training and used during testing is indicated by dashed red arrows. For the sake of clarity we have limited the number of labeled patterns to two.

### ALGORITHMS

Novelty detection using a deep ANN can be separated into three steps: 1) feature learning, 2) dimension reduction, 3) novelty evaluation. As the first step the ANN is trained under supervision, using the labeled known patterns. Afterwards a feature space is defined using all nodes, which particularly contains the ones crucial for classification. Typically, the dimension of this feature space is large. To reduce the sparse error and to improve the analyzing efficiency, one can remove the irrelevant features by *dimension reduction* which can be implemented using an autoencoder [27]. An autoencoder is an ANN with identical number of input and output nodes and hidden layers with fewer nodes. Its loss function measures the difference between input and output values, defined as the reconstruction error  $L_{\text{loss}} = \|x - x'\|^2$ . Here  $x$  and  $x'$  are the vector of input and output nodes, respectively. So the autoencoder learns unsupervised how to reconstruct its input. This allows the autoencoder to form a submanifold in the full feature space. Finally, the novelty evaluator recognizes as novel events the testing data points which are scored high. The algorithm is shown in Fig. 1. For HEP data analysis, the sample of known patterns and the data of unknown patterns are interpreted as SM background and signal events defined by BSM physics, respectively.

We generate MC data with MadGraph5\_aMC@NLO [28] and rely on Keras [29] using TensorFlow [30] for the ANN construction. We have checked that the results of all ANNs are stable against changes in the numbers of hidden layers and nodes. For the *supervised classification* of events with  $n$  four-momenta (normalised by 200 GeV) and  $l$  labeled patterns we use an ANN with  $4n$  input nodes,  $l$  output nodes, and three hidden layers with 30, 30 and 10 nodes, respectively. We use Nesterov's accelerated gradient descent optimizer [31] with a learning rate of 0.3, a learning momentum of 0.99 and a decay rate of  $10^{-4}$ .

The batch size is fixed to be 30 and the loss function is categorical cross entropy [32, 33]. The collections of all nodes constitute the feature space with dimension  $m = 4n + 30 + 30 + 10 + l$ , this ensures that it contains the non-linear information learned for classification. Note, we normalized each dimension of the feature space to  $[-1, 1]$  with *tanh* activation functions for autoencoder. Then an *autoencoder* consisting of five hidden layers with 40, 20, 8, 20 and 40 nodes, respectively, projects this feature space onto an eight-dimensional sub-space. The learning rate is changed to 2.0.

### NOVELTY EVALUATION

The novelty evaluation for testing data is a crucial step for novelty detection. Various approaches have been developed in the past decades [18]. For non-time series data, one of the most popular approaches is density-based [34], in which a Local Outlier Factor (LOF), i.e., the ratio of the local density of the given testing point and the local densities of its neighbors, is proposed as a novelty measure. Both densities are defined w.r.t. the training dataset. Explicitly, this traditional measure is [35, 36].

$$\Delta_{\text{trad}} = \frac{d_{\text{train}} - \langle d'_{\text{train}} \rangle}{\langle d'^2_{\text{train}} \rangle^{1/2}}, \quad (1)$$

with  $d_{\text{train}}$  being the mean distance of a testing data point to its  $k$  nearest neighbors,  $\langle d'_{\text{train}} \rangle$  being the average of the mean distances defined for its  $k$  nearest neighbors, and  $\langle d'^2_{\text{train}} \rangle^{1/2}$  being the standard deviation for the latter. We calculate  $\langle d'^2_{\text{train}} \rangle^{1/2}$  below using the method suggested in [35, 36]. Then the probabilistic novelty evaluator, with a shift here, is defined as  $\mathcal{O} = 0.5 \text{erf}(c\Delta) + 0.5$  with  $c$  being a normalization factor. This measure efficiently picks up the isolation of the testing data point from the training dataset. A data point located away from or at the distribution tail thus tends to get high novelty score [34, 35].

This measure however is blind to the clustering features, such as resonance and shape, of the testing points which generically exist in BSM physics. It would be helpful that this effect can be utilized for optimizing novelty evaluation. Thus we introduce a new measure:

$$\Delta_{\text{new}} = \frac{d_{\text{test}}^{-m} - d_{\text{train}}^{-m}}{d_{\text{train}}^{-m/2}}, \quad (2)$$

defined in an  $m$ -dimensional feature space. Here  $d_{\text{test}}$  represents the mean distance of the testing data point to its  $k$  nearest neighbors in the testing dataset, whereas  $d_{\text{train}}$  represents its SM prediction which can be approximately calculated using the training dataset. As  $\Delta_{\text{new}} \propto \frac{S}{\sqrt{B}}$  approximately, with  $S$  and  $B$  being the numbers of signal and background events in a local bin with unit area,

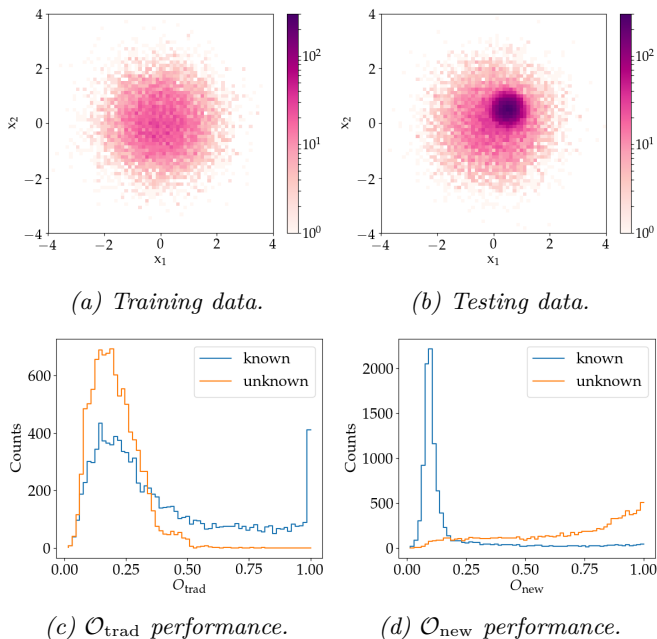


FIG. 2: Comparison of the traditional and new novelty evaluators. We show the toy-data in Panels (a) and (b) and the novelty response in (c) and (d).

this measure can be approximately interpreted as the significance of discovery, up to a calibration constant.

In order to compare the performance of the traditional and new novelty evaluators, we introduce a toy model, where the data resides in a two-dimensional space. The known pattern  $\mathcal{N}(\vec{0}, \mathbf{I})$  is a Gaussian distribution centered at the origin, while the unknown pattern  $\mathcal{N}((0.5, 0.5)^T, 0.1\mathbf{I})$  is a narrow Gaussian distribution slightly shifted from the origin. While the training dataset contains  $10^4$  events of the known pattern (FIG. 2a), the testing dataset contains  $10^4$  events from the known pattern and  $10^4$  events from the unknown pattern (FIG. 2b). Comparing FIG. 2c and FIG. 2d, we conclude that the clustering effect of the unseen class data, which is hidden from  $\Delta_{\text{trad}}$ , is well picked-up by  $\Delta_{\text{new}}$ .

Despite of this,  $\Delta_{\text{new}}$  suffers from statistical fluctuation of the known-pattern testing data, via the  $1/d_{\text{test}}^m$  term in Eq. (2). Without fluctuation, the measure values of these data should be zero, unless the testing dataset contains data of unknown patterns. With the fluctuation turned on, the data fluctuating upward will be scored high by  $\Delta_{\text{new}}$ , since it picks up local event excess, compared to the training dataset. Note, the fluctuation effect for the  $1/d_{\text{train}}^m$  term can be neglected, as long as a training dataset much larger than the testing one is used for calculating  $1/d_{\text{train}}^m$ .

This fluctuation effect can be suppressed as the luminosity  $L$  increases, if  $k$  is scaled as  $k \propto L$ . This can be understood since more data points are used to calculate  $1/d_{\text{test}}^m$  in the local bin. The suppression by luminosity

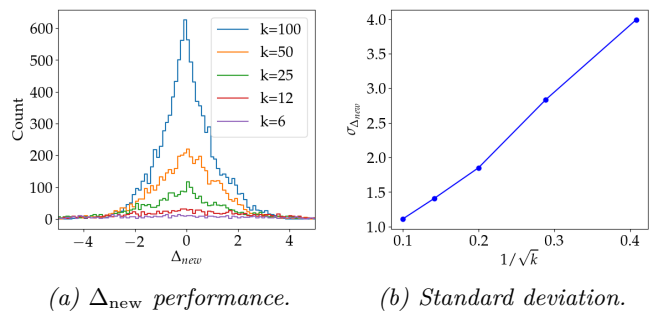


FIG. 3: Influence of statistical fluctuation in the known-pattern testing dataset for the  $\Delta_{\text{new}}$  performance, with different luminosities. Here  $k$  is scaled with luminosity.  $\sigma_{\Delta_{\text{new}}}$  is standard deviation. Its suppression by luminosity is approximately dictated by central limit theorem.

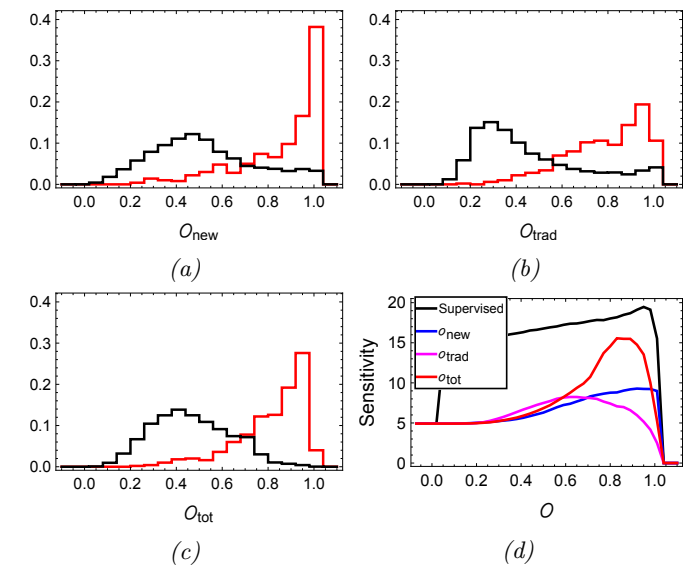


FIG. 4: Normalized responses to novelty evaluators  $\mathcal{O}_{\text{new}}$  (a),  $\mathcal{O}_{\text{trad}}$  (b), and  $\mathcal{O}_{\text{tot}}$  (c) and their sensitivity performance (d).

is approximately dictated by the central limit theorem which states that in the considered context the standard deviation for the known-pattern data response to  $\Delta_{\text{new}}$  is scaled with  $1/\sqrt{L}$ . This property is shown in Fig 3, using the Gaussian sample of known pattern defined before. The training dataset is composed of 50000 data points. The number of data points in the testing datasets are 10000, 5000, 2500, 1250 and 625, respectively.  $k$  scales linearly as 100, 50, 25, 12 and 6, respectively. As the number of testing data points increases, the corresponding distributions become gradually narrowed after normalization (see Fig. 3a). Indeed, the standard deviation  $\sigma_{\Delta_{\text{new}}}$  is scaled with  $1/\sqrt{k}$  or equivalently with  $1/\sqrt{L}$ , as is indicated in Fig. 3b.

If the fluctuation is not fully suppressed by high luminosity, some known-pattern events can still be scored high, compared to the typical  $\Delta_{\text{new}}$  response of the unknown

	Parameter values	$\sigma(fb)$
X1	$m_T = m_{\bar{T}} = 1.2 \text{ TeV}$ , $\text{BR}(T \rightarrow W_l^+ b) = 50\%$	0.152
X2	$m_{Z'} = 3 \text{ TeV}$ , $g_{Z'} = g_Z$ , $\text{BR}(Z' \rightarrow tt) = 16.7\%$	1.55
Y1	$m_{N_1} = \frac{m_{N_2}}{9} = \frac{m_a}{4} = 10 \text{ GeV}$ , $\text{BR}(h \rightarrow fs) = 1\%$	0.108
Y2	$m_a = 25 \text{ GeV}$ , $\text{BR}(h \rightarrow fs) = 1\%$	0.053

TABLE I: Parameter values and cross sections (after preselection) in the benchmark scenarios of BSM physics. “fs” denotes the final state defined in the text.

pattern which is approximately set by  $S/\sqrt{B}$  in the signal neighborhood. The sensitivity for novelty detection hence could be damaged. To compensate for this, we propose one more novelty evaluator, the geometric mean of  $\mathcal{O}_{\text{trad}}$  and  $\mathcal{O}_{\text{new}}$

$$\mathcal{O}_{\text{tot}} = \sqrt{\mathcal{O}_{\text{trad}} \mathcal{O}_{\text{new}}} . \quad (3)$$

This evaluator utilizes the fact that the known-pattern data with high novelty scores often arise from the high-density region of the feature space, whereas such data are typically scored low by  $\mathcal{O}_{\text{trad}}$ . As is indicated in Fig. 4, this novelty evaluator shows an outstanding performance in the typical case at LHC where the novelty responses for the known and unknown pattern data partially overlap with each other. The known-pattern dataset used in this analysis is the same as before, containing  $10^4$  events. The unknown pattern is defined as  $\mathcal{N}((1.5, 1.5)^T, 0.1\mathbf{I})$ , with  $S/B = 1/20$ . Indeed, compared to the novelty response of  $\mathcal{O}_{\text{new}}$  in Fig. 4a, a sizable fraction of high-score known-pattern data have been pushed to the low-score end in Fig. 4c, due to the suppression effect of  $\mathcal{O}_{\text{trad}}$  which is indicated in Fig. 4b. Eventually this complementarity results in 50% improvement in sensitivity, compared to the ones defined by  $\mathcal{O}_{\text{trad}}$  and  $\mathcal{O}_{\text{new}}$ , respectively.

## STUDY ON BENCHMARK SCENARIOS

To illustrate its performance in semi-realistic cases, next we will apply novelty detection to two analyses at parton level, with two benchmark scenarios of BSM physics defined for each. In the first analysis, we simulate the final state  $\bar{b}bl^+l^- E_T^{\text{miss}}$  at the 14 TeV LHC, with a luminosity assumption of  $L = 3 \text{ ab}^{-1}$ . We apply the preselection cuts requiring exactly two bottom quarks with  $p_T > 20 \text{ GeV}$  and two leptons with  $p_T > 10 \text{ GeV}$ . In the SM this is generated mainly via

$$\mathbf{B}_1: pp \rightarrow \bar{t}l t_l; \sigma = 11.5 \text{ fb}$$

$$\mathbf{B}_2: pp \rightarrow t_l \bar{b} W_l^\pm; \sigma = 0.365 \text{ fb}$$

$$\mathbf{B}_3: pp \rightarrow Z_b Z_l; \sigma = 0.0765 \text{ fb}$$

Note, here we have multiplied the real cross sections by a universal suppression factor 2000 for simplification. Though being unrealistic, it is sufficient for illustrating the sensitivity performance of the proposed algorithms, compared to the traditional ones. In BSM physics, this

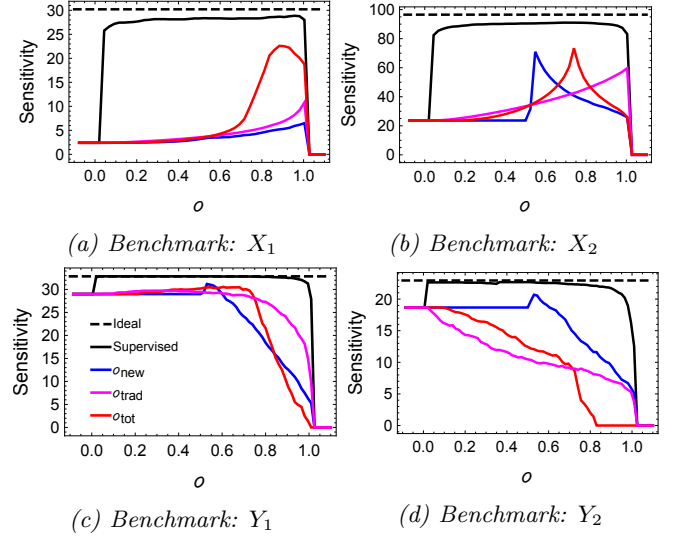


FIG. 5: Sensitivity performance of novelty detection in the benchmark scenarios.

signal could be generated in multiple scenarios. We will focus on two of them:

$\mathbf{X}_1$ :  $pp \rightarrow \bar{T}T \rightarrow W_l^+ W_l^- \bar{b}b$  where  $\bar{T}$  and  $T$  are fermionic top partners.

$\mathbf{X}_2$ :  $pp \rightarrow Z' \rightarrow \bar{t}t$  where  $Z'$  is a new gauge boson.

In the second analysis, we simulate the unpolarized  $e^+e^- \rightarrow Zh$  production with a final state  $\bar{b}bl^+l^- E_T^{\text{miss}}$  at  $\sqrt{s} = 240 \text{ GeV}$   $e^+e^-$  collider, with a luminosity assumption of  $L = 5 \text{ ab}^{-1}$ . We apply the preselection cuts requiring exactly two bottom quarks with  $p_T > 10 \text{ GeV}$  and two leptons with  $p_T > 5 \text{ GeV}$ . A systematic study on exotic Higgs decays can be found in [37]. In the SM, this is mainly generated by

$$\mathbf{B}_4: e^+e^- \rightarrow hZ \rightarrow Z_{E_T^{\text{miss}}}^* Z_b l^+ l^-; \sigma = 0.00686 \text{ fb.}$$

$$\mathbf{B}_5: e^+e^- \rightarrow hZ \rightarrow Z_b^* Z_{E_T^{\text{miss}}} l^+ l^-; \sigma = 0.00259 \text{ fb.}$$

This signal could be generated in multiple modes of exotic Higgs decay. We will focus on two of them:

$\mathbf{Y}_1$ :  $h \rightarrow N_2 N_1 \rightarrow a + 2N_1$ . This decay topology can arise from either the nearly Peccei-Quinn symmetric limit in the NMSSM [38, 39], where  $N_2$  and  $N_1$  are bino- and singlino-like neutralinos, respectively, and  $a$  is a light CP-odd scalar.

$\mathbf{Y}_2$ :  $h \rightarrow Za$  in the 2HDM and the NMSSM [37].

The parameter values and cross sections for the four benchmark scenarios of the two analyses are summarized in Tab. I.

The sensitivity performance of novelty detection is presented in Fig. 5. In each panel, one curve generated in an “Ideal” case (assuming 100% signal efficiency and 0% background efficiency) and one curve generated using supervised learning are presented. Both of them can serve as a reference point to evaluate the sensitivity performance of the novelty-detection algorithms. The toy model dis-

cussed above nicely mimics what happens in benchmark  $X_1$  at LHC. The fluctuation effect at the SM bulk in the feature space dominates over the physical background for detecting BSM physics. With a suppression resulting from the  $\mathcal{O}_{\text{trad}}$  response for such non-physical background events, sizable sensitivity improvement is achieved in the  $\mathcal{O}_{\text{tot}}$ -based detection. For benchmark  $X_2$ , the fluctuation effect is less severe for the  $\mathcal{O}_{\text{new}}$ -based detection given a large separation for many unknown-pattern events from the known-pattern data bulk in the feature space. These events can be efficiently picked up also in the  $\mathcal{O}_{\text{trad}}$ -based detection. This eventually results in comparable sensitivities for the three type of novelty-detections. As for the benchmarks  $Y_1$  and  $Y_2$  at future  $e^+e^-$  collider, the sensitivity performance of the  $\mathcal{O}_{\text{new}}$ -based detection is universally better than that of the others. This can be understood since the fluctuation effect is negligibly small for the  $\mathcal{O}_{\text{new}}$ -based detection, whereas the known-pattern and the unknown-pattern data are not fully separated, limiting the efficiency of  $\mathcal{O}_{\text{new}}$ .

## SUMMARY AND DISCUSSION

In this letter, we developed a set of density-based novelty evaluators, i.e.,  $\mathcal{O}_{\text{new}}$  and  $\mathcal{O}_{\text{tot}}$ , which can measure the clustering effect of the testing data. These novelty evaluators enable us to design novelty-detection algorithms with broader applications in HEP, compared to the traditional density-based ones, and potentially to extend their applications to other big-data domains, given that they are designed in a general context for novelty detection.

Despite of its encouraging outcomes, this study can be further generalized. We focus on the algorithm development for novelty detection, using parton-level analysis for displaying their sensitivity performance. The benchmark scenarios studied are typical. But we are also interested in other possibilities, e.g., the scenarios where there exists interference between the known and unknown patterns, or non-trivial data clustering structure like a dip. Also, the feature selection in the ANN training process might not be optimized yet. The ANN in this letter learns relevant features for representation and classification of the known-pattern dataset. These features are likely to be sub-optimal for enhancing isolation or clustering of the unknown-pattern data. Nevertheless, the algorithms developed in this letter could be further improved to reduce the performance gap with the supervised learning. For example, we may introduce dynamical ML or some feedback mechanisms in response to the testing dataset, to reinforce the feature representation. Moreover, although it is beyond the scope of this study, a full analysis of the systematic and theoretical uncertainties, which could limit the sensitivities expected, are absent (for a recent effort partially addressing this, see [40]). We leave these topics to a future study.

**[Note added]** When this paper was in finalization, the paper [41] appeared. Both the novelty evaluators proposed in this paper and the test statistic defined in [41] can measure the clustering effect of the unknown-pattern testing data. We stress that we developed the idea proposed here independently. Particularly, different from [41], we also proposed a novelty evaluator to relieve the potential negative influence of fluctuation in the known-pattern dataset for novelty detection (this fluctuation effect also exists in the context of [41]), by combing with traditional wisdom.

## Acknowledgments

We would greatly thank Prof. Michael Wong, our colleague at the HKUST, for highly valuable discussions on the novelty evaluators and the ANN algorithms which were developed in this paper. T. Liu would thank Huai-Ke Guo for discussions on central limit theorem in this context during the MITP (the Mainz Institute for Theoretical Physics) workshop “Probing Baryogenesis via LHC and Gravitational Wave Signatures”, June, 2018. We would thank Kirill Prokofiev for reading the manuscript. We would also thank Lian-Tao Wang and Zhen Liu for general discussions on this idea at an early stage. J. Hajer is partly supported by the General Research Fund (GRF) under Grant № 16304315. Y. Y. Li would thank the Kavli Institute for Theoretical Physics, where most of this work was done, for the award of the graduate fellowship which was provided by Simons Foundation under Grant № 216179 and Gordon and Betty Moore Foundation under Grant № 4310. This research was also supported in part by the National Science Foundation under Grant № NSF PHY-1748958. T. Liu is jointly supported by the GRF under Grant № 16312716 and 16302117. The GRF is issued by the Research Grants Council of Hong Kong S.A.R. He would also thank the MITP for its hospitality, where part of this work was done.

- 
- [1] A. L. Samuel, IBM Journal of Research and Development **3**, 210 (1959).
  - [2] J. R. Quinlan, Mach. Learn. **1**, 81 (1986).
  - [3] C. Peterson, T. Rögvaldsson, and L. Lönnblad, Comput. Phys. Commun. **81**, 185 (1994).
  - [4] Y. LeCun, Y. Bengio, and G. Hinton, Nature **521**, 436 (2015).
  - [5] A. Krizhevsky, I. Sutskever, and G. E. Hinton, in *Advances in Neural Information Processing Systems 25*, edited by F. Pereira, C. J. C. Burges, L. Bottou, and K. Q. Weinberger (Curran Associates, Inc., 2012) pp. 1097–1105.
  - [6] G. Hinton, L. Deng, D. Yu, G. E. Dahl, A.-r. Mohamed, N. Jaitly, A. Senior, V. Vanhoucke, P. Nguyen, T. N.

- Sainath, and B. Kingsbury, *IEEE Signal Proc. Mag.* **29**, 82 (2012).
- [7] T. Mikolov, I. Sutskever, K. Chen, G. S. Corrado, and J. Dean, in *Advances in Neural Information Processing Systems 26*, edited by C. J. C. Burges, L. Bottou, M. Welling, Z. Ghahramani, and K. Q. Weinberger (Curran Associates, Inc., 2013) pp. 3111–3119.
- [8] L. Zdeborová, *Nat. Phys.* **13**, 420 (2017).
- [9] G. Carleo and M. Troyer, *Science* **355**, 602 (2017).
- [10] J. Carrasquilla and R. G. Melko, *Nat. Phys.* **13**, 431 (2017).
- [11] P. Zhang, H. Shen, and H. Zhai, *Phys. Rev. Lett.* **120**, 066401 (2018).
- [12] P. Baldi, K. Bauer, C. Eng, P. Sadowski, and D. Whiteson, *Phys. Rev. D* **93**, 094034 (2016).
- [13] A. Butter, G. Kasieczka, T. Plehn, and M. Russell, (2017), arXiv:1707.08966 [hep-ph].
- [14] A. J. Larkoski, I. Moulton, and B. Nachman, (2017), arXiv:1709.04464 [hep-ph].
- [15] S. Macaluso and D. Shih, (2018), arXiv:1803.00107 [hep-ph].
- [16] P. Baldi, P. Sadowski, and D. Whiteson, *Nat. Commun.* **5**, 436 (2014).
- [17] T. Cohen, M. Freytsis, and B. Ostdiek, *JHEP* **02**, 034 (2018), arXiv:1706.09451 [hep-ph].
- [18] M. A. Pimentel, D. A. Clifton, L. Clifton, and L. Tarassenko, *Signal Processing* **99**, 215 (2014).
- [19] E. M. Metodiev, B. Nachman, and J. Thaler, *JHEP* **10**, 174 (2017), arXiv:1708.02949 [hep-ph].
- [20] A. Andreassen, I. Feige, C. Frye, and M. D. Schwartz, (2018), arXiv:1804.09720 [hep-ph].
- [21] T. Aaltonen *et al.* (CDF), *Phys. Rev.* **D78**, 012002 (2008), arXiv:0712.1311 [hep-ex].
- [22] “MUSIC – An Automated Scan for Deviations between Data and Monte Carlo Simulation,” (2008).
- [23] T. A. collaboration (ATLAS), (2017).
- [24] M. Kuusela, T. Vatanen, E. Malmi, T. Raiko, T. Aaltonen, and Y. Nagai, *Proceedings, 14th International Workshop on Advanced Computing and Analysis Techniques in Physics Research (ACAT 2011): Uxbridge, UK, September 5-9, 2011*, *J. Phys. Conf. Ser.* **368**, 012032 (2012), arXiv:1112.3329 [physics.data-an].
- [25] J. H. Collins, K. Howe, and B. Nachman, (2018), arXiv:1805.02664 [hep-ph].
- [26] R. T. D’Agnolo and A. Wulzer, (2018), arXiv:1806.02350 [hep-ph].
- [27] P. Vincent, H. Larochelle, Y. Bengio, and P.-A. Manzagol, in *Proceedings of the 25th International Conference on Machine Learning, ICML ’08* (ACM, New York, NY, USA, 2008) pp. 1096–1103.
- [28] J. Alwall, R. Frederix, S. Frixione, V. Hirschi, F. Maltoni, O. Mattelaer, H. S. Shao, T. Stelzer, P. Torrielli, and M. Zaro, *High Energy Phys.* **2014**, 79 (2014).
- [29] F. Chollet *et al.*, “Keras: The python deep learning library,” <https://keras.io> (2015).
- [30] M. Abadi *et al.*, “TensorFlow: Large-scale machine learning on heterogeneous systems,” <https://tensorflow.org> (2015).
- [31] Y. Nesterov, in *Doklady AN USSR*, Vol. 269 (1983) pp. 543–547.
- [32] R. Rubinstein, *Methodol. Comput. Appl.* **1**, 127 (1999).
- [33] R. Y. Rubinstein, in *Stochastic optimization: algorithms and applications* (Springer, 2001) pp. 303–363.
- [34] M. Breunig, H. Kriegel, R. Ng, and J. Sander, in *Proceedings of the ACM SIGMOD International Conference on Management of Data, SIGMOD ’00*, Vol. 29 (ACM, New York, NY, USA, 2000) pp. 93–104.
- [35] H. Kriegel, P. Kroger, E. Schubert, and A. Zimek, in *Proceedings of the 18th ACM conference on Information and knowledge management, CIKM ’09* (ACM, New York, NY, USA, 2009) pp. 1649–1652.
- [36] R. Socher, M. Ganjoo, C. D. Manning, and A. Ng, in *Advances in Neural Information Processing Systems 26*, edited by C. J. C. Burges, L. Bottou, M. Welling, Z. Ghahramani, and K. Q. Weinberger (Curran Associates, Inc., 2013) pp. 935–943.
- [37] D. Curtin *et al.*, *Phys. Rev.* **D90**, 075004 (2014), arXiv:1312.4992 [hep-ph].
- [38] P. Draper, T. Liu, C. E. M. Wagner, L.-T. Wang, and H. Zhang, *Phys. Rev. Lett.* **106**, 121805 (2011), arXiv:1009.3963 [hep-ph].
- [39] J. Huang, T. Liu, L.-T. Wang, and F. Yu, *Phys. Rev. Lett.* **112**, 221803 (2014), arXiv:1309.6633 [hep-ph].
- [40] C. Englert, P. Galler, P. Harris, and M. Spannowsky, (2018), arXiv:1807.08763 [hep-ph].
- [41] A. De Simone and T. Jacques, (2018), arXiv:1807.06038 [hep-ph].